DYNAMIC INTERACTION ANALYSIS BETWEEN HIGH-SPEED TRAIN AND MULTI-SPAN PRESTRESSED CONCRETE BOX GIRDER BRIDGES

Vo Van Hiep, Tran Le Anh Duc, Phan Hoang Nam*

The Universtiy of Danang – University of Science and Technology, Vietnam

*Corresponding author: phnam@dut.udn.vn

(Received: May 02, 2025; Revised: June 15, 2025; Accepted: June 18, 2025)

DOI: 10.31130/ud-jst.2025.23(9B).502E

Abstract - This study analyzes dynamic interaction between high-speed trains and multi-span reinforced concrete box-girder bridges, considering approach embankment stiffness and rail–bridge connection. A finite element model in Midas Civil 2024 simulates the coupled train–rail–bridge system using Eurocode-based train and equivalent-rail representations. Parametric analyses across ranges of embankment stiffness and connection rigidity identify modeling parameters. Subsequently, time-history dynamic analyses are performed on a continuous prestressed concrete box-girder bridge to quantify responses under multiple train velocities. The dynamic impact factor is evaluated for critical components and compared against international provisions to assess applicability to Vietnamese conditions. Results highlight sensitivity of bridge responses to boundary stiffness transitions and connection rigidity, and delineate parameter ranges that limit vibration and amplification at high speed. The study recommends an optimal configuration for approach stiffness and rail–bridge connection, providing a technical basis for safe and efficient design of high-speed railway bridges in Vietnam.

Key words - Dynamic interaction analysis; time history analysis method; finite element method; high-speed railway bridges; Eurocode

1. Introduction

The rapid development of high-speed railway systems worldwide, particularly in advanced economies, has introduced new technical challenges in the design and evaluation of bridge structures. Unlike conventional road or traditional railway bridges, high-speed railway bridges must meet stricter dynamic stability standards due to complex dynamic load effects from trains operating at speeds exceeding 200 km/h. Factors such as structural vibrations, resonance phenomena, and uneven load distribution can amplify stress concentrations, potentially compromising structural stability if not adequately addressed during design [1]. Neglecting or inaccurately assessing these dynamic factors may not only lead to miscalculations of load-bearing capacity but also impair long-term serviceability and pose critical safety risks to trains and passengers during operation.

In Vietnam, as the North-South High-Speed Rail Project undergoes pre-feasibility studies, the need for precise analytical and simulation models to evaluate train-bridge interaction has become more urgent than ever. Such models are essential to ensure technical feasibility and optimize designs for local conditions, including terrain characteristics, climate, and operational requirements. While international standards like Eurocode [2], AREMA [3], and JRA [4] provide methodologies for calculating dynamic amplification factor (DAF) and detailed guidelines for assessing bridge dynamic behavior under high-speed train loads, these standards were developed based on infrastructure and operational environments in advanced economies. Their applicability to Vietnam with unique material properties, construction techniques, and loading regimes requires further validation through localized research.

High-speed railway systems impose unprecedented demands on bridge design and evaluation. Unlike conventional bridges, high-speed rail bridges must satisfy rigorous dynamic stability criteria due to intense dynamic loads from trains operating above 200 km/h. Overlooking dynamic effects can lead to design inaccuracies, reduced service life, and operational safety hazards. As Vietnam advances pre-feasibility studies for its North-South High-Speed Rail line, developing accurate train-bridge interaction models is imperative. Although international standards (e.g., Eurocode [2], AREMA [3] or JRA [4]) offer DAF calculation methods, their suitability for Vietnam's specific conditions remains unverified. This study focuses on the dynamic analysis of high-speed railway bridges, aiming to establish a localized database and propose design solutions tailored to domestic operational requirements.

In high-speed rail systems, when trains exceed 200 km/h, the excitation frequency of moving loads may approach or coincide with the bridge's natural vibration frequency. This elevates resonance risks, which can induce excessive oscillations, critically compromising structural stability [5]. Thus, resonance analysis and mitigation are mandatory in high-speed rail bridge design. Eurocodes (a primary reference for Vietnam's railway bridge standards) – stipulate dynamic analysis requirements via a decision flowchart in Figure 1 (EN 1991-2-6.4.4), evaluating key parameters: maximum train speed (V, km/h), span length (L, m), fundamental bending frequency (n_0, Hz), fundamental torsional frequency (n_T, Hz), nominal peak velocity (v, m/s), and the limit ratio $(v/n_0)_{lim}$ per EN 1991-2:2003 Annex F. For bridge structures subjected to train speeds exceeding 200 km/h, and especially for multi-span continuous bridges as discussed in this study, conducting dynamic analysis is essential to ensure the accuracy in evaluating the structural behavior.

The dynamic analysis in this study was conducted based on the characteristic parameters of actual trainsets

expected to operate on the North–South high-speed railway line in Vietnam, or alternatively, on the standardized HSLM (high-speed load model) recommended for high-speed railways with potential international traffic connectivity [6]. A direct time history analysis method was employed to simulate and evaluate the dynamic behavior of the bridge structure under the influence of moving trains. This method enables a detailed reproduction of the interaction process between the dynamic loads induced by trains and the bridge's structural response over time, thereby providing a comprehensive understanding of structural performance under various operating conditions.

To illustrate the applicability of the proposed method, the study conducted an analysis on a specific case involving a high-speed railway bridge structure proposed by the Tedi–Tricc–Tedisouth [7] consultancy joint venture under the framework of the North–South high-speed railway project. The computational results not only confirmed the feasibility of the analysis method but also provided critical data regarding vibrations, stresses, and strains of the bridge under dynamic loading. These results are of high practical relevance and serve as a valuable reference for further studies on the dynamic analysis of high-speed railway bridges in Vietnam. Furthermore, the research contributes to the development of a scientific basis for adapting design standards to local conditions, supporting the planning and implementation of the high-speed railway project, while ensuring operational safety and efficiency in the future.

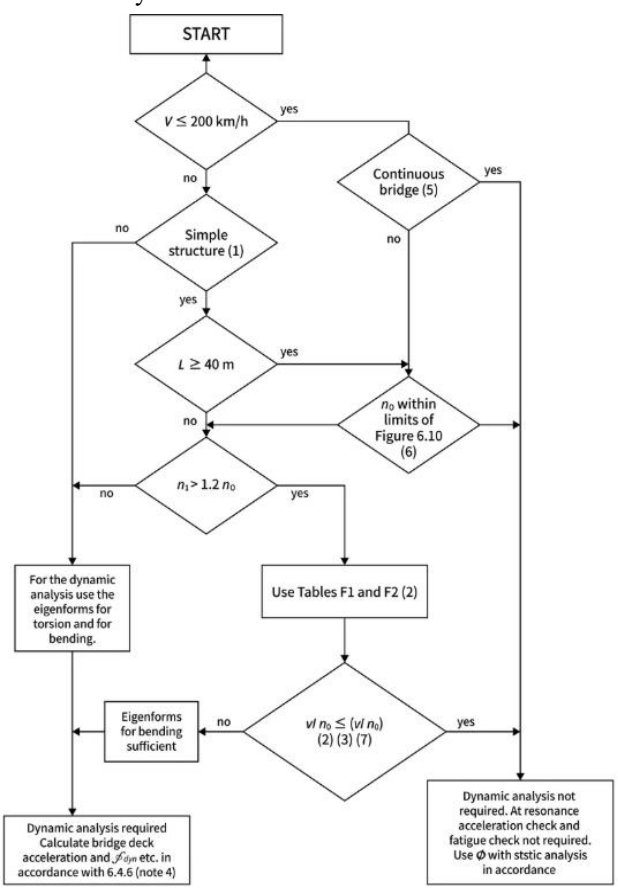

Figure 1. *Flowchart for checking the necessity of conducting dynamic analysis according to Eurocodes (EN 1991-2-6.4.4)*

2. Time history dynamic analysis method

The time history analysis method is a widely adopted numerical approach in structural dynamics, particularly suitable for assessing the response of structures subjected to dynamic loads such as those induced by moving trains. This method enables the simulation of a structure's time-dependent behavior, including displacements, velocities, accelerations, and internal forces - under the influence of temporally varying loads. In railway applications, train loads are modeled as moving forces, and the system's equations of motion are solved using numerical integration schemes.

One of the key advantages of time history analysis is its ability to capture nonlinear behavior and resonance effects, which are especially important for high-speed railway bridges operating at velocities exceeding 200 km/h. In this study, the method is applied to investigate the train–bridge interaction, thereby supporting optimized structural design and ensuring operational safety under realistic loading scenarios.

The general form of the dynamic equilibrium equation in time history analysis is expressed as:

$$[\mathrm{M}]\ddot{u}(\mathrm{t}) + [\mathrm{C}]\dot{u}(\mathrm{t}) + [\mathrm{K}]\mathrm{u}(\mathrm{t}) = \mathrm{p}(\mathrm{t}) \quad (1)$$

where $[M]$ is the mass matrix of the structure, $[C]$ is the damping matrix, representing the level of vibration attenuation, $[K]$ is the stiffness matrix, characterizing the structural resistance, and $p(t)$ is the dynamic load acting on the structure at time t. $\ddot{u}(t), \dot{u}(t), u(t)$ represent the acceleration, velocity, and displacement of the structure at time t, respectively.

The implementation of time history analysis typically follows these steps [8]:

Step 1: Initialization

Specify initial conditions for displacement $u(0)$ and velocity $\dot{u}(0)$ at time $t = 0$.

Step 2: Time discretization

Divide the total simulation time into small intervals of length Δt. The choice of Δt must ensure numerical stability and adequately capture the dynamic response.

Step 3: Time-stepping calculation

At each discrete time step $t_i = i\Delta t$, determine the corresponding load $p(t_i)$. Solve the system of equations to compute the displacement u_i, velocity $\dot{u}i$, and acceleration $\ddot{u}i$ of the structure.

Step 4: Iterative computation

Use the results from the current time step as the basis for calculating the response in the next step. Repeat this process iteratively until the simulation reaches the final analysis time.

The time history analysis method plays a crucial role in the design and evaluation of high-speed railway bridge structures, where structural vibrations directly impact the safety and smoothness of train operations. This method is also accepted and recommended for use by the Eurocode and many other high-speed railway bridge design standards worldwide.

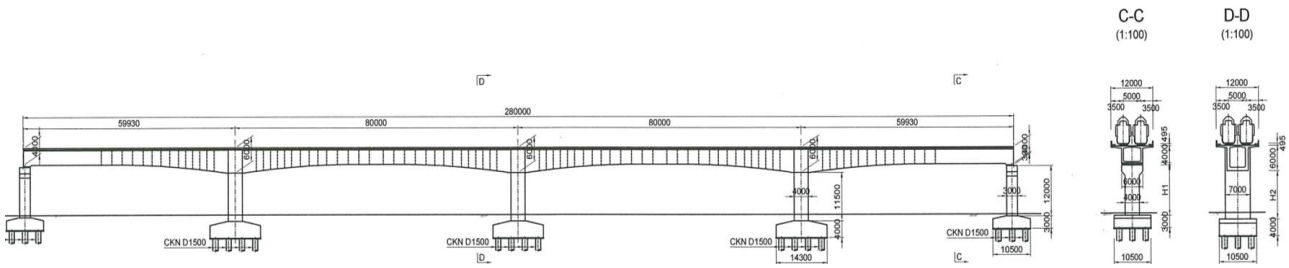

Figure 2. *Typical structure of box girder bridge with spans of 60 – 80 – 80 – 60 meters of the North–South high-speed railway project (Pre-feasibility study stage)*

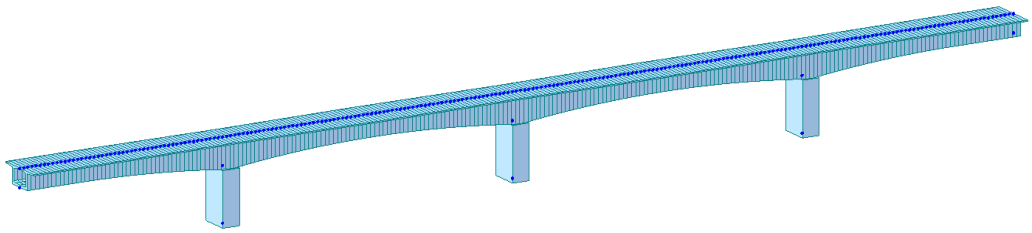

Figure 3. *Finite element model of prestressed concrete box girder bridge structure with 60–80–80–60 m spans of the North–South high-speed railway project (Pre-feasibility study stage)*

3. Applying analysis to the structure of a multi-span reinforced concrete box girder bridge

In this study, the time history dynamic analysis method was applied to a high-speed railway bridge structure proposed by the TEDI–TRICC–TEDIS consultancy joint venture during the pre-feasibility phase of the North–South High-Speed Railway project. The selected structure is an elevated bridge utilizing a prestressed concrete box girder (PCBC) system with a continuous span configuration of 60–80–80–60 meters. The general layout and cross-sectional geometry of the bridge are illustrated in Figure 2.

The bridge features a total width of 12 meters, accommodating two standard-gauge railway tracks (1.435 meters) and designed for a maximum operating speed of up to 350 km/h.

It is important to note that, at the time of this study, the North–South High-Speed Railway project remains in the pre-feasibility research stage, and no official documents have been published regarding the dynamic analysis of this specific bridge structure. As such, the present analysis is conducted independently and does not form part of the project's official assessment.

3.1. Bridge model

The bridge structure was modeled using the finite element method and analyzed with MIDAS/Civil 2024 software. The superstructure was represented using spatial beam elements, with a uniform element length of 1 meter to ensure sufficient resolution. Variable cross-section properties were assigned to simulate the geometry of the prestressed concrete box girder and supporting columns.

Support conditionswere modeled to reflect realistic boundary behavior: the bearings at the tops of the piers were modeled as rigid links to simulate full rotational restraint, while the bearings at both abutments were represented as roller supports to allow longitudinal displacement. The mass properties of the superstructure were modeled as lumped masses and assigned at the nodal points of the beam elements. The complete structural model developed in MIDAS/Civil is illustrated in Figure 3.

3.2. Track model

The rail system is modeled using two primary components: an equivalent rail beam representing the continuous rail profile, and a series of elastic spring-damper elements simulating the interaction between the rail beam and the bridge deck.

3.2.1. Rail (UIC60)

The train is modeled as a moving load traveling along the bridge structure, with the load applied directly to a single beam element. To accurately simulate the dynamic interaction between the train and the bridge, the two actual rails are idealized as a single equivalent rail beam. This conversion ensures that the mechanical behavior and load transfer characteristics of the system are properly captured within the structural model. The equivalent rail beam is designed to preserve the essential mechanical properties of the original dual-rail system, including the cross-sectional area, moment of inertia, and material properties, thereby maintaining the fidelity of the train–bridge interaction simulation.

When performing the conversion, the main parameters that need to be recalculated include:

Total cross-sectional area:

$$A_{new} = 2A_{single} \tag{2}$$

where A_{new} là is the cross-sectional area of the equivalent rail, and A_{single} is the cross-sectional area of a single original rail.

Moment of inertia about the vertical axis (I_{yy}) using the Parallel axis theorem:

$$I_{yy,new} = 2I_{yy,single} + 2A_{single}\left(\frac{d}{2}\right)^2 \tag{3}$$

where $I_{yy,new}$ is the new moment of inertia (after merging two rails), $I_{yy,single}$ is the moment of inertia of a single original

rail, A_{single} is the cross-sectional area of a single original rail, and d is the distance between the two rails (center to center).

Moment of inertia about the horizontal axis (I_{xx}) and the vertical axis (I_{zz}):

$$A_{xx,new} = 2A_{xx,single}$$
$$A_{yy,new} = 2A_{yy,single} \quad (4)$$

Since the two rails are placed parallel to each other along the horizontal axis, the values of I_{xx} and I_{zz} are simply the sum of the moments of inertia of the two individual rails.

Table 1. *Comparison between the parameters of an individual rail and an equivalent rail*

Parameter	Unit	One rail	Two rails converted into one equivalent rail
Cross-sectional area (A)	m²	0.0153389	0.0306778
Moment of inertia (I_{xx})	m⁴	4.33934e-06	8.67868e-06
Moment of inertia (I_{yy})	m⁴	6.07260e-05	1.5915e-02
Moment of inertia (I_{zz})	m⁴	1.02091e-05	2.04182e-05
Young's modulus (E)	kN/m²	2.1×10^8	2.1×10^8
Poisson's ratio		0.3	0.3
Coefficient of thermal expansion	1/[°C]	0.000001	0.000001
Density	kN/m³	78.5	78.5

Based on the above formulas, the comparison table between the parameters of a single rail and the equivalent rail after conversion is presented in Table 1.

3.2.2. Elastic link between the rail and the bridge deck

Since we are only concerned with the behavior of the bridge and rail when the train passes, the connections between the equivalent rail and the bridge deck are modeled using elastic link elements, representing the stiffness of intermediate components such as rail clips, cushioning layers, and the support system.

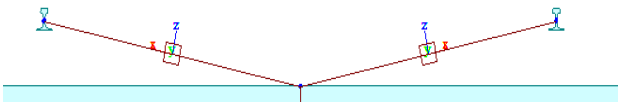

Figure 5. *The elastic link connection model between the rail element and the bridge deck along the horizontal axis of the bridge*

The optimal stiffness value is selected based on the analysis process, and the vertical stiffness for the model is chosen as 10^6 (KN/m) for the ballastless track.

3.3. Model of the bridge approach

The embankment foundation at the bridge approach is modeled as nodes with different vertical spring stiffnesses (point spring supports) based on the allowable settlement according to the reference standard. According to the Eurocode for high-speed railway bridges in Europe, the maximum allowable settlement is 25 mm.

Figure 6. *Bridge approach embankment model*

Table 2. *Table of soil foundation stiffness values in the vertical direction*

Settlement S (mm)	Support reaction at the abutment F_z (KN)	Stiffness K_z (KN/m)
5mm	531.5	106300
10mm	531.5	53150
15mm	531.5	35433
20mm	531.5	26575
25mm	531.5	21260

3.4. Train model

According to the Eurocode standards, when performing dynamic analysis for high-speed railway bridges with speeds V >200 km/h, the characteristic parameters of the actual trains expected to be operated or the HSLM train model should be used. For routes with the potential for international connectivity, 10 HSLM-A train models (from A1 to A10) can be applied, with detailed parameters presented in Figure 6 and Table 3.

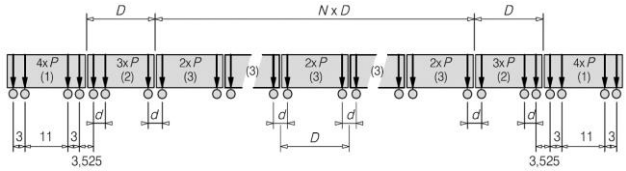

Figure 7. *The HSLM-A train model*

Table 3. *Parameters of the HSLM-A Train Load Model*

Universal Train	Number of intermediate coaches N	Coach length D [m]	Bogie axle spacing d [m]	Point force P [kN]
A1	18	18	2.0	170
A2	17	19	2.5	200
A3	16	20	2.0	180
A4	15	21	3.0	190
A5	14	22	2.0	170
A6	13	23	2.0	180
A7	13	24	2.0	190
A8	12	25	2.5	190
A9	11	26	2.0	210
A10	11	27	2.0	210

4. Analysis results

4.1. Effects of the rail-bridge connection stiffness

To assess the influence of rail–bridge connection stiffness on the structural response, a series of simulations were conducted by varying the connection stiffness across a wide range while monitoring the resulting internal forces in both the bridge and rail.

As shown in Table 4 and Figures 8-10, when the connection stiffness is high, the rail and bridge exhibit nearly uniform movement, allowing most of the dynamic load from the train to be directly transmitted to the bridge structure. Conversely, with lower connection stiffness, the rail is able to oscillate independently within the elastic range of the connection, allowing a significant portion of

the dynamic load to be absorbed by the rail and elastic interface components. This reduces the direct load transferred to the bridge and mitigates vibrations. These observations indicate that selecting an appropriate connection stiffness is critical for optimizing load distribution and minimizing vibrations in the bridge structure under high-speed train loads.

According to the UIC 774-3 standard, EN 1991-2, and supporting experimental studies, the rail moment under high-speed train loading typically ranges from 10–30 kN·m. Based on the analysis results, the optimal connection stiffness for high-speed railway bridges lies within the range of 7.5×10^4 to 1×10^6 kN/m, ensuring an effective balance between minimizing vibrations and efficiently transferring loads to the bridge structure [9].

Table 4. *The effect of the connection stiffness between the rail and the bridge on the internal forces*

Stiffness (kN/m)	Beam moment (kN.m)		Rail moment (kN.m)	
	Pier	Span	Negative	Positive
10000	-10807.0	4335	-28.0	54.0
25000	-10805.7	4336.3	-23.2	40.7
50000	-10805.8	4344	-20.4	32.7
75000	-10805.8	4346.8	-18.9	28.9
100000	-10805.8	4348	-19.3	26.7
250000	-10805.7	4352	-17.5	21.5
500000	-10805.5	4353.4	-16.9	19.3
750000	-10805.4	4354	-17.1	18.5
1000000	-10805.8	4355.5	-17.0	18.0
2500000	-10805.1	4359.5	-17.3	17.5
5000000	-10805.5	4361.6	-17.5	17.5
7500000	-10805.7	4362.5	-17.5	17.2
10000000	-10805.8	4363	-17.4	17.0

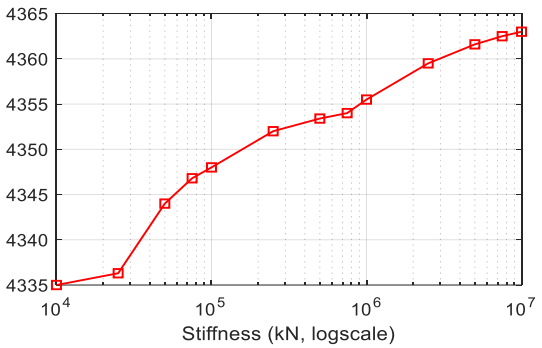

Figure 8. *Relationship between stiffness and moment at mid-span*

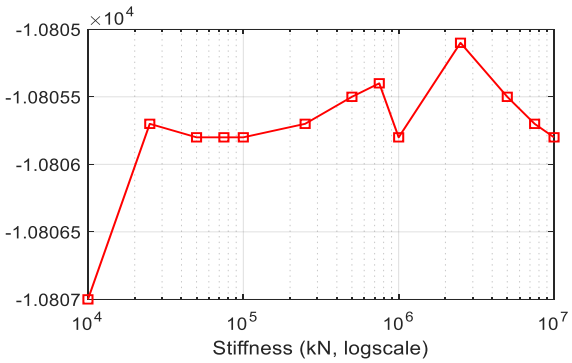

Figure 9. *Relationship between stiffness and moment at the pier top*

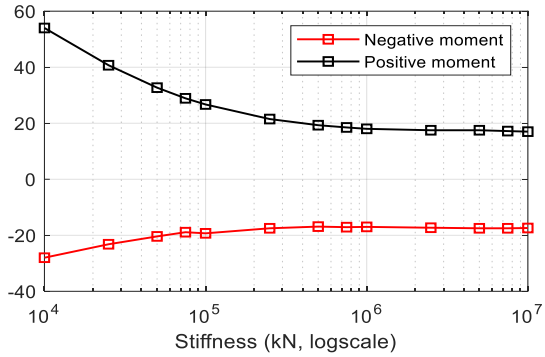

Figure 10. *Relationship between stiffness and moment in the rail*

4.2. Effects of the bridge approach settlement

To evaluate the influence of settlement at the bridge approach on the structural response, a series of simulations were conducted by incrementally increasing the allowable settlement levels while monitoring the corresponding changes in shear force within the bridge structure. The analysis considered settlement values ranging from 5 mm to 25 mm, which align with typical allowable limits specified in design standards for high-speed railway bridges. For each settlement case, the corresponding stiffness of the foundation was adjusted, and the resulting support reactions and maximum shear forces were recorded to assess the sensitivity of the bridge's response to approach settlement variations.

The results in Table 5 and Figure 11 indicate that as the stiffness of the bridge approach decreases (due to increasing settlement), the maximum shear force in the bridge shows a slight increase. However, this variation remains minimal across the examined settlement range. Therefore, it can be concluded that bridge approach settlement has an insignificant impact on the bridge's dynamic response, provided that settlement remains within the allowable design limits.

Table 5. *Effect effect of the bridge approach settlement on the shear force*

Settlement S (mm)	Support reaction at the bridge end support F_z (kN)	Stiffness K (kN/m)	Shear force Max (F_{zmax}) (kN)
5	531.5	106300	-838.51
10	531.5	53150	-838.58
15	531.5	35433	-838.62
20	531.5	26575	-838.65
25	531.5	21260	-838.67

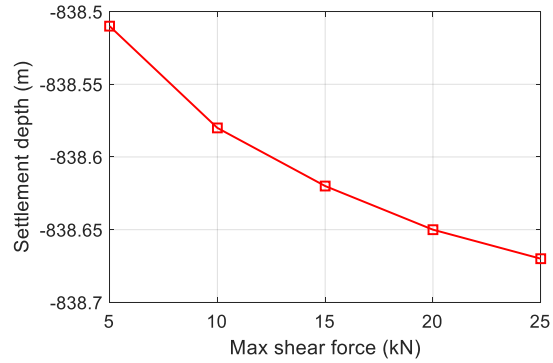

Figure 11. *Relationship between the allowable settlement depth and the shear force*

4.3. Results of dynamic analysis

4.3.1. Eigenvalue analysis

During train passage, the bridge structure experiences forced vibrations at the excitation frequencies induced by the moving train loads. Once the train has passed, the bridge transitions to free vibrations at its natural frequencies. To accurately evaluate the dynamic response of the structure, it is essential to perform eigenvalue analysis to determine the natural frequencies, mode shapes, and mass participation factors associated with each vibration mode. These parameters are influenced by the structural configuration, mass distribution, and the required accuracy and computational capacity of the analysis.

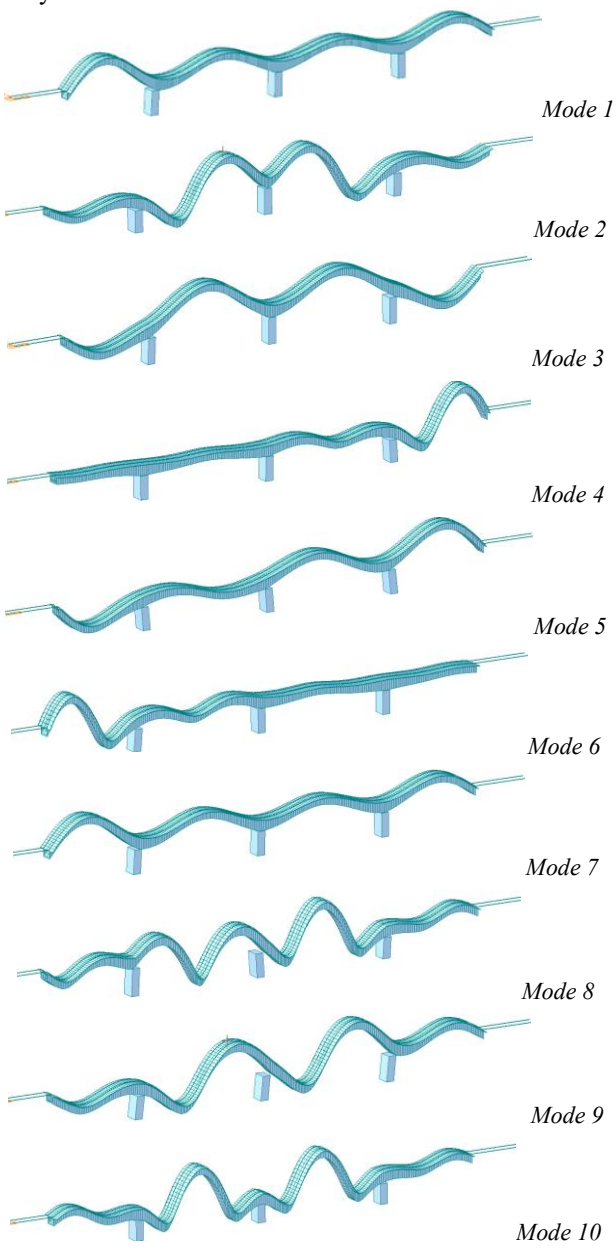

Figure 12. *The first 10 vibration modes of the span structure*

As shown in Figure 12, Mode 4 (6.043 Hz) exhibits a mass participation factor of 46.73% in the D_z (vertical) direction, indicating that this mode is dominant for vertical (longitudinal bending) vibrations of the bridge. Meanwhile, Mode 3 (5.424 Hz) has a mass participation factor of 44.89%, highlighting its significant contribution to torsional vibrations of the bridge structure under high-speed train loading.

4.3.2. Time history analysis

According to the Eurocode standards, time history analysis is performed by modeling the moving concentrated load of the train. This load is applied at the nodal points on the model at the center of the rail and changes over time, depending on the velocity, as well as the distance between consecutive nodes.

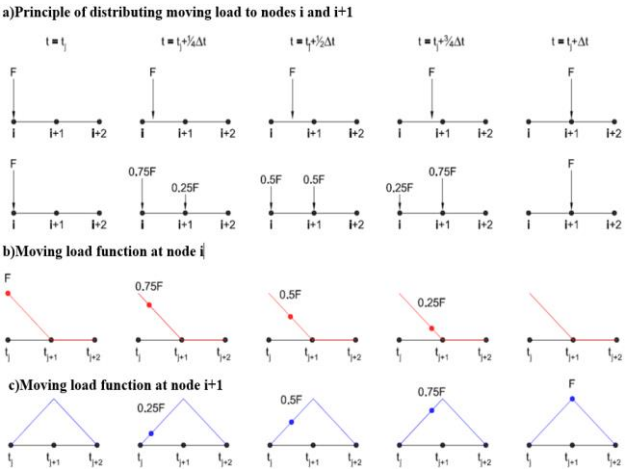

Figure 13. *Principle for establishing time-dependent load functions at node i and i + 1*

Principle of load distribution is shown in Figure 13, in particular:

- As a wheel axle moves across two elements sharing a node i, the force applied to this node is distributed based on the ratio between the distance from the load application point and the length of the element being loaded.

- The forces applied to nodes i and i + 1 are similarly distributed, as illustrated in Figure 12.

An example of the load-time function at the beam's leading node (node 1) and another node located 10 meters away (node 10) is shown in Figure 14, with load amplitudes corresponding to the wheel axle loads.

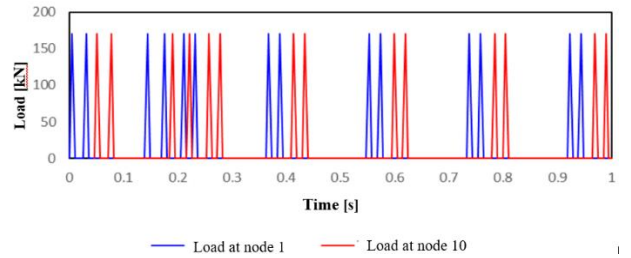

Figure 14. *Illustration of constructing the time-dependent load function applied to Node 1 and Node 10 at a train speed of v = 350 km/h during the first second*

To ensure the accuracy of the finite element model in dynamic analysis of high-speed railway bridges using the time history method, two critical factors must be considered:

- Damping ratio: According to Eurocodes, a viscous damping ratio of ξ=1.0% may be assumed for prestressed concrete bridges with span lengths greater than 20 m [2], [6].

- Time step (Δt): The smaller the time step, the more accurate the calculation results - but the computational time increases. According to the recommendation of the European Rail Research Institute (ERRI) [10], Δt should be smaller than the minimum of the following quantities:

$$h_1 = 1/8fmax;\ h_2 = Lmin/(200v);$$

$$h_3 = Lmin/(4nv);\ h_4 = 0.001s$$

where f_{max} is the highest natural frequency used in the modal analysis, n is the number of vibration modes included in the analysis, v is the train speed.

In this case study, a time step of Δt = 0.001 s is used in the dynamic simulations.

4.3.3. Analysis results

Dynamic analysis (1) was carried out using the HSLM-A1 train model. The analysis was performed at different speeds ranging from a minimum of 200 km/h up to 420 km/h (1.2 times the design speed V_{tk} = 350 km/h according to Eurocodes) with increments of 25 km/h. Key vibration response results of the bridge under live load from the HSLM-A1 train are presented at the location with the highest response (the fourth pier from the right for internal forces, and midspan for displacements). The internal force and displacement results are shown in Figures 15-17.

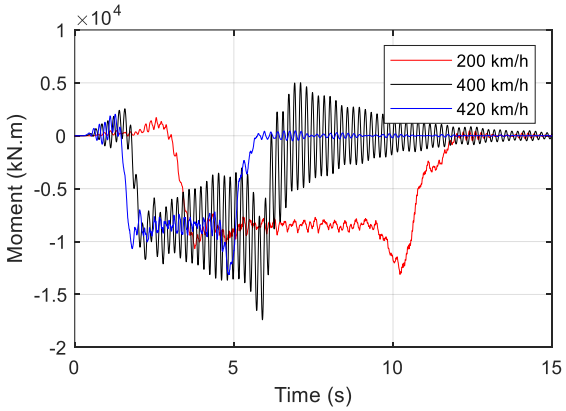

Figure 15. *Moment at Pier 4 under the action of HSLM-A1 train passing at varying speeds of 200, 350, and 420 km/h*

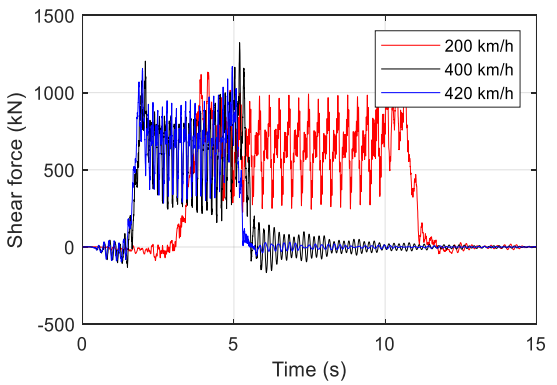

Figure 16. *Shear force at Pier 4 under the action of HSLM-A1 train passing at varying speeds of 200, 400, and 420 km/h*

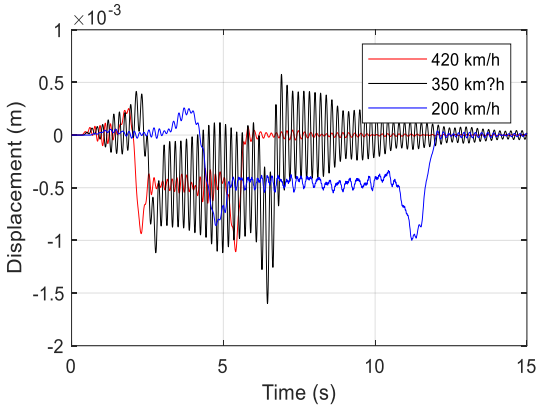

Figure 17. *Displacement at mid-span under the action of HSLM-A1 train passing at speeds of 200, 350, and 420 km/h*

Dynamic analysis (2) was conducted using 10 HSLM trains (HSLM-A1 to HSLM-A10), each running over the bridge at the design speed of 350 km/h.

The structural responses of the bridge were converted into dynamic amplification factors, which serve as the basis for comparison and evaluation in accordance with current design standards. The value of the dynamic amplification factor is determined as follows:

$$\varphi'_{dym} = max\,[y_{dyn}/y_{stat}] \quad (5)$$

where y_{dym} is the maximum dynamic response, y_{stat} is the maximum static response.

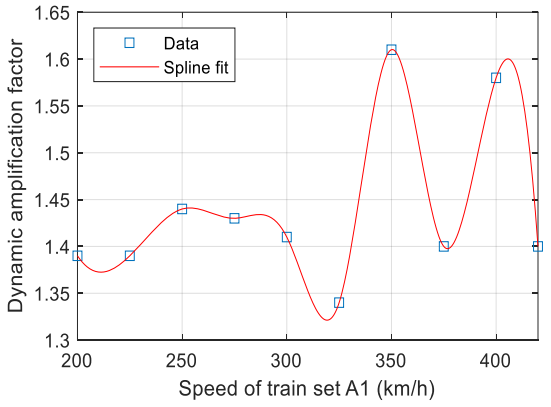

Figure 18. *Diagram of the relationship between varying speeds of an HSLM-A1 train and the dynamic amplification factor*

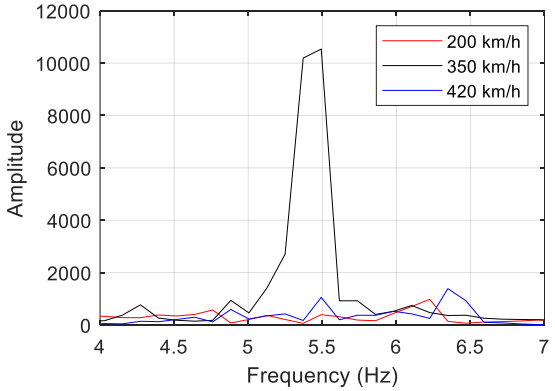

Figure 19. *The oscillation amplitude of the bending moment at Pier T4 due to train-induced excitation*

As shown in Figure 18, the significant increase in the dynamic amplification factor at the speed of 350 km/h is attributed to a sudden spike in the bridge's vibration amplitude as the train passes Pier T4. This phenomenon occurs because the excitation frequency of the train coincides with the natural frequency of 5.4 Hz associated with Mode 3 (Figure 19), which is characterized by rotational motion around the horizontal axis (R_y = 44.89%). The resulting resonance induces substantial torsional vibrations, leading to a pronounced increase in the structural dynamic response.

The surge in the dynamic amplification factor at the speed of 400 km/h is caused by the bridge reaching a high vibration amplitude as the train moves over Pier T4. This occurs due to the excitation frequency of the train coinciding with the natural frequency of 6.043 Hz associated with Mode 4 (Figure 20), which corresponds to vertical bending motion (D_z = 46.73%). This resonance significantly amplifies the vertical oscillations, thereby intensifying the dynamic response of the structure.

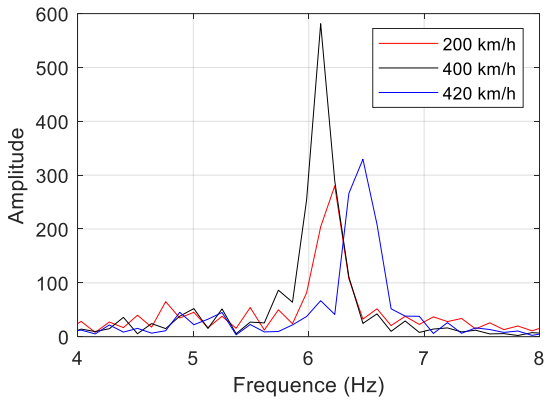

Figure 20. *The oscillation amplitude of the shear force at Pier T4 due to train-induced excitation*

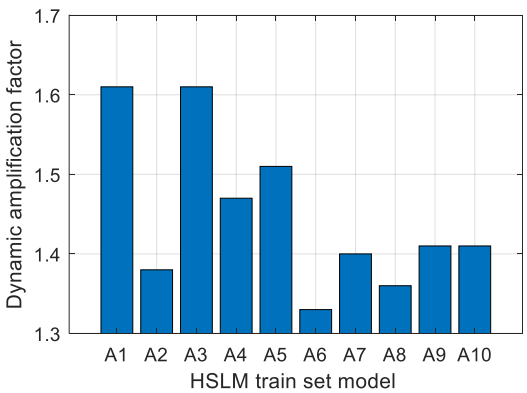

Figure 21. *Dynamic amplification factor of the bridge with 10 HSLM-A trains at 350Km/h*

The analysis indicates that train speed alone has a limited effect on the DAF. Instead, the primary influence on DAF arises when the train's excitation frequencies coincide with the bridge's natural frequencies, leading to resonance and amplified structural responses.

Figure 21 shows the DAF values for the bridge under the action of 10 different HSLM-A train models operating at 350 km/h. The results reveal no clear increasing or decreasing trend in DAF across the A1 to A10 train models, demonstrating that each train exhibits distinct dynamic characteristics. Parameters such as the number of carriages, car length, axle spacing, and axle loads have only a minor impact on the DAF, while resonance remains the dominant factor driving amplification under high-speed train loading.

4.4. Comparison of DAF values corresponding to different speeds of the HSLM-A1 train with current standards in various countries

4.4.1. Japan Railway Standards (JRA)

The dynamic amplification factor generally remains within the permissible range (1.1 – 1.4) at speeds below 325 km/h. However, at speeds of 350 km/h and 400 km/h, the factor exceeds the maximum threshold specified by JRA, reaching values of 1.61 and 1.58 respectively [4].

4.4.2. American Standards (AREMA)

AREMA does not specify an explicit limit for the dynamic amplification factor but requires a design review if the factor exceeds 1.5. At speeds of 350 km/h and 400 km/h, the dynamic amplification factor surpasses this warning threshold [3].

4.4.3. Russian Standards (SNIP 2.05.03-84)

The dynamic amplification factor ranges from 1.3 to 1.6, which is in line with SNIP at most speeds. At 350 km/h, the dynamic amplification factor reaches 1.61, slightly exceeding the maximum threshold [11].

5. Conclusions

This study applied the time history dynamic analysis method to evaluate the dynamic response of multi-span prestressed concrete box girder bridges under high-speed train loads, using a detailed finite element model that incorporates realistic rail–bridge interaction and train load representations. The analysis was performed on a bridge structure proposed for Vietnam's North–South High-Speed Railway, providing valuable insights for its future design and implementation. The key conclusions are as follows:

The DAF is not solely dependent on train speed but is significantly influenced by resonance phenomena. At train speeds of 350 km/h and 400 km/h, the excitation frequencies of the moving train align with the bridge's natural frequencies (Mode 3 at 5.42 Hz and Mode 4 at 6.04 Hz), resulting in substantial amplification of torsional and vertical oscillations, respectively.

Analysis across the 10 standardized HSLM-A train models revealed no consistent trend in DAF variation among different configurations, indicating that bridge dynamic responses are more sensitive to the train's dynamic loading characteristics (e.g., axle load frequency spectrum) than to basic geometric parameters such as the number of carriages or axle spacing.

The calculated DAF values generally remain within the permissible limits of international design codes, including

JRA (Japan), AREMA (USA), and SNIP (Russia), under most operational speeds. However, exceedances were observed at critical resonance speeds, underscoring potential vulnerabilities if resonance effects are not carefully considered during the design stage.

These findings confirm that resonance is a dominant factor impacting the safety and serviceability of high-speed railway bridges. To mitigate associated risks, the following engineering strategies are recommended:

- Modifying bridge geometry and material properties to increase stiffness and shift the natural frequencies away from the excitation frequency ranges typical of high-speed train operations.

- Considering the incorporation of tuned mass dampers, viscous dampers, or other energy dissipation devices to effectively reduce resonance-induced vibrations.

The results serve as a valuable reference for validating and adapting international dynamic load standards to the specific context of Vietnam's high-speed railway infrastructure, supporting evidence-based design adjustments for local conditions.

REFERENCES

[1] T. L. A. Duc, P. H. Nam, N. V. My, T. D. Quang, and F. Paolacci, "2D train-track-bridge interaction analysis considering the effect of ballasted tracks", *The University of Danang - Journal of Science and Technology,* vol. 22, no. 11B, pp. 1-7, 2024.

[2] *Eurocode 1: Actions on Structures – Part 2: Traffic Loads on Bridges*, BS EN 1991-2:2003, European Committee for Standardization, Brussels, Belgium, 2003.

[3] *Manual for Railway Engineering*, AREMA, American Railway Engineering and Maintenance-of-Way Association, Lanham, MD, USA, 2023.

[4] *Specifications for Highway Bridges, Part V: Seismic Design*, JRA, Japan Road Association, Tokyo, Japan, 2002.

[5] X. He, T. Wu, Y. Zou, Y. F. Chen, H. Guo, and Z. Yu, "Recent developments of high-speed railway bridges in China", *Structure and Infrastructure Engineering,* vol. 13, no. 12, pp. 1584-1595, 2017.

[6] *Railway Bridge Design with gauge 1435 mm, speed up to 350 km/h - Part 1: General Requirements*, TCVN 13594-1:2022, Ministry of Science and Technology, Ha Noi, Viet Nam, 2022.

[7] TEDI-TRICC-TEDIS, "Pre-feasibility study report of high-speed railway project on the North-South axis", Consultancy Consortium TEDI-TRICC-TEDIS, Ha Noi, Viet Nam, 2019.

[8] H. Xia and N. Zhang, "Dynamic analysis of railway bridge under high-speed trains", *Computers & Structures,* vol. 83, no. 23-24, pp. 1891-1901, 2005.

[9] A. K. Chopra, *Dynamics of structures: theory and applications to earthquake engineering,* 3rd ed, Pearson, London, England, 2007.

[10] *Track/Bridge Interaction – Recommendations for Calculations*, UIC 774-3, Paris, France, 2009.

[11] *Ponts-Rails pour vitesses > 200 km/h; Final report - Part B: Proposition de fiche*, UIC 776-2R, Paris, France,1999.

[12] *Bridges and Culverts*, SNIP 2.05.03-84, S. Union, 1984.